

Comparison of Sparse Adaptive Filters for Underwater Acoustic Channel Equalization/Estimation

Konstantinos Pelekanakis and Mandar Chitre

Acoustic Research Laboratory
Tropical Marine Science Institute
National University of Singapore
Singapore, 119223

E-mail: costas, mandar@arl.nus.edu.sg

Abstract—High-rate underwater acoustic (UWA) channels often demonstrate long, time-varying and sparse impulse responses. Classical and most used adaptive algorithms such as the recursive least-squares (RLS) algorithm and the normalized least-mean-square (NLMS) algorithm do not take sparseness into account when they try to match the channel. Thus, performance improvement of these algorithms is possible. Sparse adaptive algorithms developed for acoustic echo cancellation, such as the improved proportionate normalized least-mean-square (IPNLMS) algorithm and the improved proportionate affine projection algorithm (IPAPA), have shown better performance than the NLMS algorithm without any essential cost in computational complexity. In this work, we apply IPNLMS, IPAPA, RLS and NLMS in both channel estimation and decision feedback equalization (DFE) of a short-range, shallow water acoustic link. Our results confirm the superior performance of the sparse algorithms (IPAPA being the best) when the channel becomes sparse. In addition, it is shown that both IPAPA and IPNLMS have robust performance (similar to RLS) when the channel is non-sparse.

I. INTRODUCTION

In high-rate underwater acoustic (UWA) communications, long (order of 100 taps) and time-varying impulse responses are often encountered in shallow water horizontal links [1]. In addition, these impulse responses are sparse [2]. By sparse, we mean that a big fraction of their energy is concentrated in a small fraction of their duration. The long and time-varying nature of these responses causes the classical adaptive algorithms such as the recursive least-squares (RLS) algorithm and the normalized least-mean-square (NLMS) algorithm to demonstrate poor performance when they try to match these channels. The poor performance can be seen in two aspects: (a) slow convergence of the filter taps to their steady state values since the convergence rate of the algorithm is proportional to the total filter length; (b) high steady state misadjustment due to the estimation noise that inevitably occurs during the adaptation of the so-called inactive filter taps (i.e., taps with zero or close to zero values at steady-state) [3]. Since both RLS and NLMS do not exploit the sparse structure of the channel, achieving better performance seems possible. Recently, advances in sparse signal decomposition has received great

attention in UWA communications (see [4] and references therein).

Another application that deals with long (order of 1000 taps) and sparse impulse responses is acoustic echo cancellation [5]. Traditionally, the NLMS algorithm and the affine projection algorithm (APA) (APA can be regarded as an intermediate algorithm between NLMS and RLS in terms of both performance and complexity [3]) have been the workhorses in adaptive echo cancellation. Since neither NLMS nor APA can exploit sparsity, sophisticated versions such as the improved proportionate NLMS (IPNLMS) algorithm [6] and the improved proportionate APA (IPAPA) [7] were introduced. The important feature of IPNLMS and IPAPA is the "proportionate updating concept", namely, at every iteration of the algorithm, each filter tap is assigned a combination of a fixed and a variable step size parameter. The variable step size parameter is a function of the tap's previously estimated magnitude. As a result, active filter taps (i.e., taps with significant values at steady-state) converge fast, which makes the overall algorithm to have fast initial convergence since the active taps contribute more to the overall error than the inactive taps. The fixed step size parameter makes the algorithms to have robust performance in non-sparse channels. In fact, it was shown that IPAPA and IPNLMS always have better performance than their non-proportionate counterparts APA and NLMS, respectively, no matter how sparse the channel is [6], [7].

In this paper, we apply IPNLMS, IPAPA, RLS and NLMS using experimental data recorded over a short-range, shallow water channel. The performance of the above algorithms is evaluated in terms of initial convergence rate and misadjustment in a channel estimation experiment. Moreover, these algorithms are used for adapting a decision feedback equalization (DFE) receiver in a communications experiment. Bit-error-rate (BER) results are reported.

Notation: Superscripts \top , \dagger , and $*$ stand for transpose, Hermitian transpose, and conjugate, respectively. Column vectors (matrices) are denoted by boldface lowercase (uppercase) letters. $E[\cdot]$ denotes mathematical expectation, $\text{Im}\{x\}$ is the imaginary part of the complex number x , and $\|\mathbf{x}\|_1$ is the

1-norm of the L -tap vector \mathbf{x} , defined as $\|\mathbf{x}\|_1 = \sum_{i=0}^{L-1} |x_i|$.

II. PROPORTIONATE UPDATE ADAPTIVE DFE

In adaptive estimation of sparse channels, improved performance is possible if the step-size parameter of each filter tap is regulated so that the active filter taps converge faster than the inactive ones. This will increase the convergence rate since the active taps contribute more to the overall error. The underlying concept of "proportionate updating" is that each filter tap is assigned a variable step-size parameter, which is a function of the taps's magnitude [5]. Below, we review IPNLMS and IPAPA in the DFE context.

Let the vector $\mathbf{h}_{ff}(k)$ of length N_{ff} and the vector $\mathbf{h}_{fb}(k)$ of length N_{fb} denote the feedforward filter and the feedback filter of the DFE, respectively. Here, k is the time index. A fractionally-spaced DFE coupled with carrier-phase tracking is mathematically described as follows [8]:

$$e(k) = d(k) - \hat{d}(k) \quad (1)$$

$$\hat{d}(k) = p(k) - q(k) \quad (2)$$

$$p(k) = \mathbf{h}_{ff}(k)^\dagger \mathbf{u}(k) e^{-j\theta(k)} \quad (3)$$

$$q(k) = \mathbf{h}_{fb}(k)^\dagger \mathbf{d}(k) \quad (4)$$

$$\theta(k) = \theta(k-1) + K_1 \Phi(k) + K_2 \sum_{i=0}^k \Phi(i) \quad (5)$$

$$\Phi(k) = \text{Im} \{p(k)(d(k) + q(k))^*\} \quad (6)$$

$$\mathbf{u}(k) = [u(kT + N_1 T_s) \dots u(kT - N_2 T_s)]^\top \quad (7)$$

$$\mathbf{d}(k) = [d(k-1) \dots d(k - N_{fb})]^\top \quad (8)$$

where $d(k)$ denotes the transmitted/decided symbol when the DFE operates in training/decision-directed mode, $\hat{d}(k)$ is the symbol estimate, $e(k)$ is the error signal, $p(k)$ is the output of the feedforward filter, $q(k)$ is the output of the feedback filter, $\theta(k)$ is the carrier-phase estimate, K_1, K_2 are phase tracking parameters, $\Phi(k)$ is the phase detector output, $\mathbf{u}(k)$ is the received (baseband) signal vector of length $N_{ff} = N_1 + N_2 + 1$, $1/T_s$ is the sampling rate of the received signal, $1/T$ is the symbol rate, and $\mathbf{d}(k)$ is a vector containing the N_{fb} previously decided symbols. The DFE parameters $\mathbf{h}_{ff}(k)$ and $\mathbf{h}_{fb}(k)$ are computed recursively such that the mean squared error (MSE), defined as $E \left[|e(k)|^2 \right]$, is minimized.

The IPNLMS algorithm was derived by Benesty and Gay[6] for sparse channel estimation in acoustic echo cancellation applications. In the DFE framework, the recursive equations of $\mathbf{h}_{ff}(k)$ and $\mathbf{h}_{fb}(k)$ take the form:

$$\mathbf{h}_{ff}(k) = \mathbf{h}_{ff}(k-1) + \mu \frac{\mathbf{G}_{\mathbf{h}_{ff}}(k-1) \mathbf{u}(k) e(k)^*}{\mathbf{u}(k)^\dagger \mathbf{G}_{\mathbf{h}_{ff}}(k-1) \mathbf{u}(k) + \delta_{ff}} \quad (9)$$

$$\mathbf{h}_{fb}(k) = \mathbf{h}_{fb}(k-1) - \mu \frac{\mathbf{G}_{\mathbf{h}_{fb}}(k-1) \mathbf{d}(k) e(k)^*}{\mathbf{d}(k)^\dagger \mathbf{G}_{\mathbf{h}_{fb}}(k-1) \mathbf{d}(k) + \delta_{fb}} \quad (10)$$

where $\mu \in [0, 1]$ is a step-size constant, δ_{ff}, δ_{fb} are regularization parameters, and $\mathbf{G}_{\mathbf{h}_{ff}}(k), \mathbf{G}_{\mathbf{h}_{fb}}(k)$ are diagonal matrices

which depend on the filters $\mathbf{h}_{ff}(k), \mathbf{h}_{fb}(k)$, respectively. For an L -tap filter $\mathbf{h}(k)$, the diagonal entries of the matrix $\mathbf{G}_{\mathbf{h}}(k)$ are given by [6]

$$g_i(k) = \frac{1-\beta}{2L} + (1+\beta) \frac{|h_i(k)|}{2\|\mathbf{h}(k)\|_1 + \epsilon}, 0 \leq i \leq L-1 \quad (11)$$

where ϵ is a small constant to avoid division by zero and $\beta \in [-1, 1]$ is the parameter that controls the weighting between the non-proportionate and the proportionate adaptation. Note that when $\beta = -1$, the update equations (9) and (10) reduce to the NLMS algorithm.

The IPAPA was introduced by Hoshuyama *et al* [7]. In the DFE context, the recursive equations of $\mathbf{h}_{ff}(k)$ and $\mathbf{h}_{fb}(k)$ equations for the M th-order IPAPA can be written as

$$\begin{aligned} \mathbf{h}_{ff}(k) &= \mathbf{h}_{ff}(k-1) + \mu \mathbf{G}_{\mathbf{h}_{ff}}(k-1) \mathbf{U}(k) \times \\ &\quad (\mathbf{U}(k)^\dagger \mathbf{G}_{\mathbf{h}_{ff}}(k-1) \mathbf{U}(k) + \delta_{ff} \mathbf{I})^{-1} \mathbf{e}(k) \end{aligned} \quad (12)$$

$$\begin{aligned} \mathbf{h}_{fb}(k) &= \mathbf{h}_{fb}(k-1) - \mu \mathbf{G}_{\mathbf{h}_{fb}}(k-1) \mathbf{D}(k) \times \\ &\quad (\mathbf{D}(k)^\dagger \mathbf{G}_{\mathbf{h}_{fb}}(k-1) \mathbf{D}(k) + \delta_{fb} \mathbf{I})^{-1} \mathbf{e}(k) \end{aligned} \quad (13)$$

$$\mathbf{e}(k) = \bar{\mathbf{d}}^*(k) - (\mathbf{U}(k)^\dagger \mathbf{h}_{ff}(k) - \mathbf{D}(k)^\dagger \mathbf{h}_{fb}(k)) \quad (14)$$

$$\mathbf{U}(k) = [\mathbf{u}(k) e^{-j\theta(k)} \dots \mathbf{u}(k-M+1) e^{-j\theta(k-M+1)}] \quad (15)$$

$$\mathbf{D}(k) = [\mathbf{d}(k) \dots \mathbf{d}(k-M+1)] \quad (16)$$

$$\bar{\mathbf{d}}(k) = [d(k) \dots d(k-M+1)]^\top \quad (17)$$

where $\mathbf{e}(k)$ is the $M \times 1$ error signal vector, the small numbers δ_{ff}, δ_{fb} and the identity matrix \mathbf{I} are used for regularization, $\mathbf{U}(k)$ is the $N_{ff} \times M$ matrix of output signal samples, and $\mathbf{D}(k)$ is the $N_{fb} \times M$ matrix of input signal symbols. The \mathbf{G} matrices are the same as in the IPNLMS algorithm. Note again that when $\beta = -1$, the above equations reduce to the standard APA.

III. EXPERIMENTAL RESULTS

The experimental data were recorded in the area of Selat Pauh in Singapore waters on April 21st, 2010. Both the transmitter and the receiver were mounted on rigid tripods, 4m above the sea floor. The sea depth was 15m and the horizontal range of the link was 350m. The sound speed profile was isovelocity 1540m/s and the sea surface was calm during the experiment. The transmitted signal was a 5kbps rate, BPSK modulated m-sequence. The m-sequence was shaped at the transmitter by a square-root cosine filter with roll-off factor 0.25 and truncation length ± 5 bit intervals. The carrier frequency was 27.5 kHz. The m-sequence served a dual purpose: (1) as a probing signal for channel impulse response estimation; (2) as a communications signal for DFE application. The received average SNR was 11.5 dB. A special feature of this channel was a broadband interference arriving

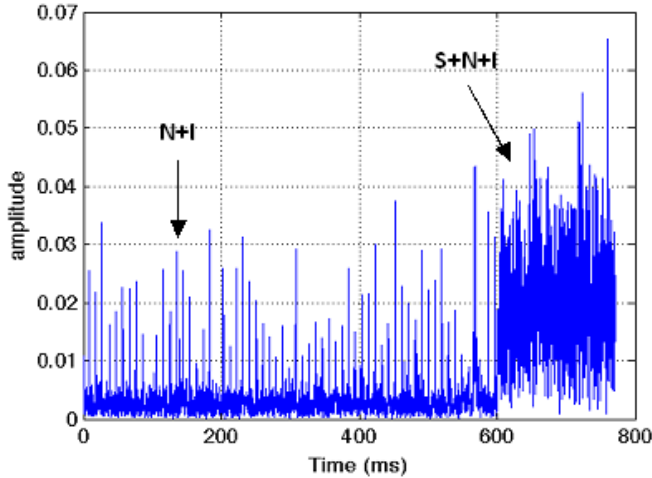


Fig. 1. A portion of the received signal. The "N+I" label shows noise plus interference. The "S+N+I" shows the signal contaminated by noise plus interference.

every 10 ms at the receiver. A segment of the baseband received signal illustrating the interference can be seen in Fig.1.

A. Adaptive Channel Estimation

We first focus on estimating the channel impulse response and compare the performances of the IPNLMS, IPAPA, RLS, and NLMS algorithms in terms of speed of convergence and steady-state misadjustment. The channel estimation problem is equivalent to the adaptive equalization problem, thus we omitted the mathematics for brevity. Here, in brief, the adaptive filter is driven by the m-sequence and tries to capture the time-varying multipath structure of the channel.

Fig. 2 illustrates the temporal evolution of the amplitude of the estimated channel impulse response over a 4 s interval using the RLS algorithm. Clearly, the total delay spread doesn't exceed 7 ms (35 taps) for this link geometry. The relatively stable tap values denoted as "D" are determined by both the direct and the first bottom-bounce sound rays. This is due to the fact that their path delay difference is less than 0.2 ms, which is the maximum delay resolution of the m-sequence. The tap values denoted as "SB" are determined by the first surface bouncing ray. The cluster of taps shown at around 2 ms delay correspond to rays that hit the bottom and the sea surface once before reaching the receiver. The cluster of taps shown at around 4 ms delay correspond to rays that hit the bottom and the sea surface twice before arriving at the receiver.

Fig. 3 shows the average mean square error (MSE) versus the number of bit intervals (learning curve) for each algorithm. Clearly, RLS converges faster and shows lower misadjustment than all other three algorithms. Specifically, RLS needs 100 ms (500 bits) to converge to -42.3 dB while IPAPA, IPNLMS, and NLMS converge to -41.5 dB, -41 dB and -40.4 dB, respectively. In addition, RLS shows -42.5 dB steady state

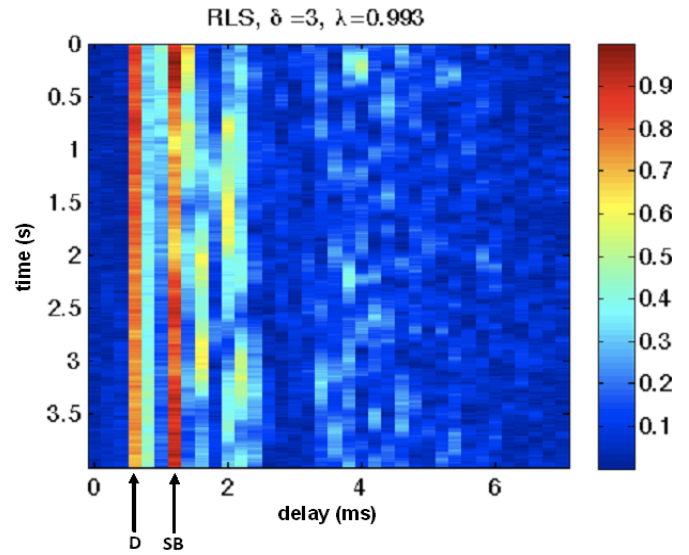


Fig. 2. Snapshots of the estimated time-varying channel impulse response using RLS algorithm. The horizontal axis represents delay, the vertical axis represents absolute time and the colorbar represents the amplitude. The intensity ranges linearly from 0 to 1.

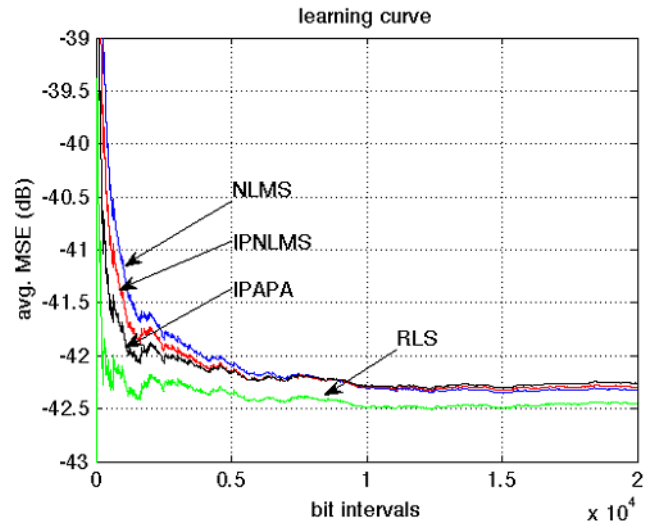


Fig. 3. Learning curves for NLMS, IPNLMS, IPAPA, and RLS when the adaptive filter has 35 taps.

misadjustment, about 0.2 dB better than the rest of the algorithms. These results imply that the channel is not sparse enough, which motivates us to increase the number of filter taps to 200. This increase does not violate the generality of the problem because a good measure of sparseness should not depend on the sorting order of the channel response taps. Note that 200 filter taps correspond to a channel of 40 ms delay spread, which is very likely to encounter in medium-range, shallow water links [1],[9].

Fig. 4 illustrates the learning curves of each algorithm for the extended channel. IPAPA shows the fastest convergence rate taking 100 ms to converge to -41.5 dB compared to

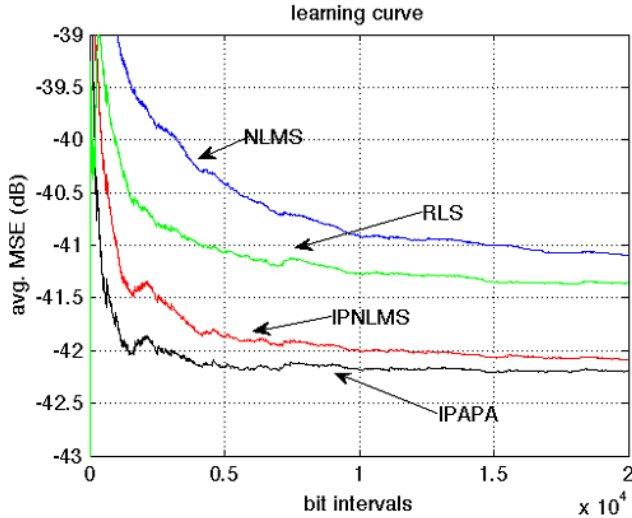


Fig. 4. Learning curves for NLMS, IPNLMS, IPAPA, and RLS when the adaptive filter has 200 taps.

TABLE I

	parameters (35-tap filter)	parameters (200-tap filter)
NLMS	$\mu = 0.3, \delta_{NLMS} = 0.001$	$\mu = 0.3, \delta_{NLMS} = 0.001$
IPNLMS	$\beta = 0, \mu = 0.3$	$\beta = 0.5, \mu = 0.3$
IPAPA	$M = 2, \beta = -0.5, \mu = 0.2$	$M = 2, \beta = 0.5, \mu = 0.3$
RLS	$\lambda = 0.993, \delta_{RLS} = 3$	$\lambda = 0.993, \delta_{RLS} = 3$

−40.2 dB, −39.4 dB and −38.4 dB for IPNLMS, RLS, and NLMS, respectively. In addition, IPAPA shows the smallest misadjustment, −42.2 dB compared to −42 dB, −41.3 dB, and −41 dB for IPNLMS, RLS, and NLMS, respectively. Note that the misadjustment for both IPAPA and IPNLMS remains the same as in Fig. 3 while the misadjustment for RLS and NLMS is increased by 1 dB each. These results confirm that: (a) IPAPA exhibits better performance than IPNLMS at a small cost of increased computational complexity; (b) RLS and NLMS are not suitable to match UWA channels with sparse structure.

Table I summarizes the algorithm parameters used to generate the learning curves in Figs. 3 and 4. Note that when the filter taps are increased from 35 to 200, parameter β is also increased so that both IPAPA and IPNLMS better capture sparseness. For clarity, we mention here that λ and δ_{RLS} are the forgetting factor and the regularization parameter, respectively, for the RLS algorithm [3]. In addition, μ and δ_{NLMS} are the step-size parameter and a small positive constant to avoid division by zero, respectively, for the NLMS algorithm.

B. Adaptive DFE

We now report on the performance of a receiver, which employs a fractionally-spaced DFE coupled with carrier-phase synchronization. DFE adaptation is performed by using the above algorithms. We compute the BER and the output

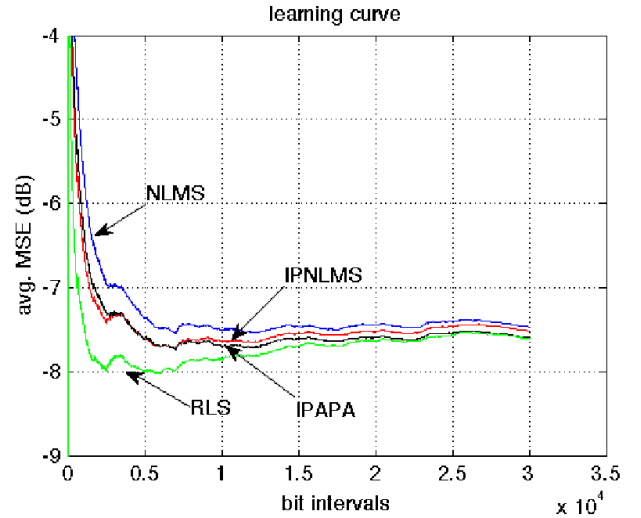


Fig. 5. Learning curves for NLMS, IPNLMS, IPAPA, and RLS when the adaptive DFE has $N_{ff} = 73$ and $N_{fb} = 35$.

SNR of the DFE, denoted as SNR_{out}^1 , which is a measure of how efficiently the DFE removes the intersymbol interference. For all the results, 500 bits out of 3×10^4 bits were used for training the DFE. Again, two scenarios are considered: a 7 ms delay spread channel and a 20 ms delay spread channel.

Fig. 5 shows the learning curve of each adaptive DFE when $N_{ff} = 73$ and $N_{fb} = 35$ (7 ms delay spread channel). Clearly, RLS demonstrates the fastest initial convergence taking 500 bits to converge to −6.7 dB as opposed to −5.3 dB, −4.9 dB, and −4.1 dB for IPNLMS, IPAPA, and NLMS, respectively. Although RLS converges faster than IPAPA, both algorithms achieve the same misadjustment, −7.6 dB.

The carrier-phase estimate can be seen in Fig. 6. The linear phase drift is due to a small mismatch between the transmitter and the receiver clocks. We noticed that the sampling rate at the receiver was about 3 Hz faster than that at the transmitter. Despite the sampling clock mismatch, there was no need for explicit bit-delay estimation during the interval of 3×10^4 bits. For brevity, we omit the plot of the carrier-phase estimate for the 20 ms channel because it is almost the same as Fig. 6.

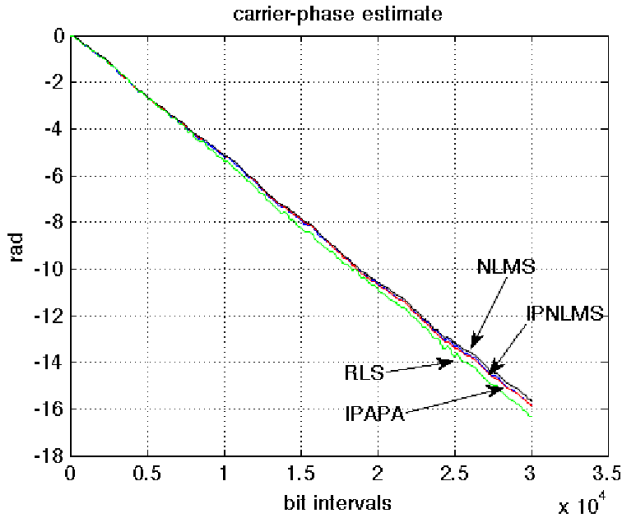
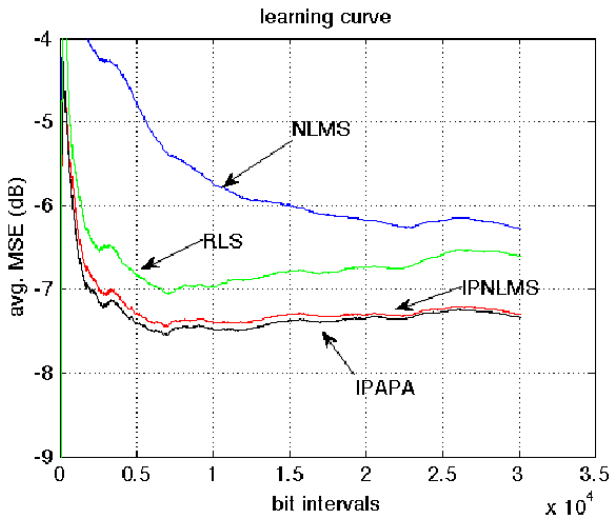
Fig. 7 illustrates the learning curve of each adaptive DFE when $N_{ff} = 203$ and $N_{fb} = 100$ (20 ms delay spread channel). After 500 bits, IPAPA and IPNLMS converge to −5.2 dB and −5.1 dB, respectively. Moreover, their misadjustment is about −7.3 dB and thus, only 0.3 dB worse than the previous scenario. Note that both RLS and LMS show slower convergence rate and higher misadjustment than the sparse adaptive algorithms due to their inability to cope with noise enhancement. For example, after 500 bits, RLS and NLMS demonstrate about 1 dB and 2.7 dB higher MSE than IPAPA, respectively.

Table II summarizes our findings for all the algorithms

$$^1SNR_{out} = 10 \log_{10} \frac{E[|d(k)|^2]}{\frac{1}{N} \sum_{k=1}^N |d(k) - \hat{d}(k)|^2} \quad [8]$$

TABLE II

	BER	SNR_{out} (dB)	parameters
$N_{ff} = 73, N_{fb} = 35$ (7 ms)			
NLMS	0.00403	7.50	$\mu = 0.2, \delta_{ff} = 0.001, \delta_{fb} = 1$
IPNLMS	0.00380	7.51	$\beta = 0, \mu = 0.2, \delta_{ff} = 4.6 \times 10^{-6}, \delta_{fb} = 4.6 \times 10^{-3}$
IPAPA	0.00325	7.60	$M = 2, \beta = 0, \mu = 0.1, \delta_{ff} = 10^{-4}, \delta_{fb} = 0.1$
RLS	0.00312	7.60	$\lambda = 0.996, \delta_{ff} = 0.01, \delta_{fb} = 10$
$N_{ff} = 203, N_{fb} = 100$ (20 ms)			
NLMS	0.01386	6.19	$\mu = 0.3, \delta_{ff} = 0.001, \delta_{fb} = 1$
IPNLMS	0.00431	7.28	$\beta = 0.5, \mu = 0.2, \delta_{ff} = 4.6 \times 10^{-6}, \delta_{fb} = 4.6 \times 10^{-3}$
IPAPA	0.00393	7.46	$M = 3, \beta = 0.5, \mu = 0.1, \delta_{ff} = 10^{-4}, \delta_{fb} = 0.1$
RLS	0.00654	6.57	$\lambda = 0.998, \delta_{ff} = 0.01, \delta_{fb} = 10$

Fig. 6. Carrier-phase estimate when the adaptive DFE has $N_{ff} = 73$ and $N_{fb} = 35$.Fig. 7. Learning curves for NLMS, IPNLMS, IPAPA, and RLS when the adaptive DFE has $N_{ff} = 203$ and $N_{fb} = 100$.

in terms of BER and SNR_{out} . For the 7 ms delay spread channel, RLS shows a slightly better performance than IPAPA in terms of BER. When the delay spread is extended to 20 ms, the sparse algorithms outperform both RLS and NLMS. Moreover, IPAPA slightly outperforms IPNLMS. These results verify that both IPAPA and IPNLMS are appropriate for practical implementations due to their robust performance in both scenarios despite the impulsive interference.

IV. CONCLUSION

Inspired by the proportionate updating concept used in acoustic echo cancellation applications, two sparse adaptive algorithms, IPNLMS and IPAPA were reviewed and applied in the context of UWA channel equalization/estimation. These algorithms were compared with the standard RLS and NLMS algorithms over a sparse and a non-sparse UWA channel. The results confirm the robust performance of the sparse algorithms in both channels and the clear superiority of the IPAPA in the sparse channel. The application of the proportionate updating concept in the RLS algorithm or a more sophisticated update rule will be pursued in future publications.

REFERENCES

- [1] D. B. Kilfoyle and A. B. Baggeroer, "The state of the art in underwater acoustic telemetry," *IEEE J. Oceanic Eng.*, vol. 25, pp. 4-27, 2000.
- [2] W. Li and J. C. Preisig, "Estimation of rapidly time-varying sparse channels," *IEEE J. Ocean. Eng.*, vol. 32, no. 4, pp. 927-939, 2007.
- [3] S. Haykin, *Adaptive Filter Theory*, 4th Ed., Prentice-Hall, Englewood Cliffs, NJ, 2002.
- [4] C. R. Berger *et al.*, "Sparse channel estimation for multicarrier underwater acoustic communication: from subspace methods to compressed sensing," *IEEE Trans. Signal Processing*, vol. 8, no. 3, pp. 1708-1721, 2010.
- [5] Y. Huang, J. Benesty, and J. Chen, *Acoustic MIMO Signal Processing*. Berlin, Germany: Springer-Verlag, 2006.
- [6] J. Benesty and S.L. Gay, "An improved PNLMS algorithm", *IEEE ICASSP-02*, vol. 2, pp. 1881-1884, May 2002.
- [7] O. Hoshuyama, R. A. Goubran, and A. Sugiyama, "A generalized proportionate variable step-size algorithm for fast changing acoustic environments," *IEEE ICASSP-04*, vol. 4, pp. 161-164, May 2004.
- [8] M. Stojanovic, J. A. Catipovic and J. G. Proakis, "Phase-coherent digital communications for underwater acoustic channels," *IEEE J. Oceanic Eng.*, vol. 19, pp. 100-111, 1994.
- [9] B. Tomasi *et al.*, "Experimental study of the space-time properties of acoustic channels for underwater communications," in *Proc. IEEE/OES Oceans*, Sydney, Australia, May 2010.